HHS Public Access

Author manuscript

J Vasc Res. Author manuscript; available in PMC 2018 November 01.

Published in final edited form as:

J Vasc Res. 2018 ; 55(1): 1–12. doi:10.1159/000484086.

Angiotensin II Infusion Does Not Cause Abdominal Aortic Aneurysms in Apolipoprotein E-Deficient Rats

Evan H. Phillips[1], **Mandy S. Chang**[1], **Sydney Gorman**[1], **Hamna J. Qureshi**[1], **Karin F. K. Ejendal**[1], **Tamara L. Kinzer-Ursem**[1], **A. Nicole Blaize**[1,2], and **Craig J. Goergen**[1,3,*]

[1]Weldon School of Biomedical Engineering, 206 South Martin Jischke Drive, Purdue University, West Lafayette, Indiana, 47907, United States

[2]Department of Health and Kinesiology, 800 West Stadium Avenue, Purdue University, West Lafayette, Indiana, 47907, United States

[3]Purdue Center for Cancer Research, 201 South University Street, Purdue University, West Lafayette, Indiana, 47907, United States

Abstract

The apolipoprotein E-deficient mouse model has advanced our understanding of cardiovascular disease mechanisms and experimental therapeutics. This spontaneous model recapitulates aspects of human atherosclerosis and allows for the development of dissecting abdominal aortic aneurysms when combined with angiotensin II. We characterized apolipoprotein E-deficient rats and hypothesized that, similar to mice, they would develop dissecting abdominal aortic aneurysms.

We created rats with a 16-basepair deletion of the apolipoprotein E gene using transcription activator-like effector nucleases. We imaged the suprarenal aorta for 28 days after implantation of miniosmotic pumps that infuse angiotensin II (200 ng/kg/min). Blood pressure, serum lipids and lipoproteins, and histology were also analyzed.

These rats did not develop pathological aortic dissection, but we did observe a decrease in circumferential cyclic strain, a rise in blood pressure, and microstructural changes in the aortic medial layer. We also measured increased serum lipids with and without high fat diet administration but did not detect atherosclerotic plaques.

Chronic infusion of angiotensin II did not lead to formation of dissecting abdominal aortic aneurysms or atherosclerosis in the rats used in this study. While reduced amounts of atherosclerosis may explain this resistance to dissecting aneurysms, further investigation is needed to fully characterize species-specific differences.

Keywords

Abdominal aortic aneurysm; Angiotensin II; Atherosclerosis; Biomechanics; Blood flow; Hypertension; Lipids and Lipoproteins; Rat; Ultrasound; Vascular diseases

[*]Correspondence should be addressed to CJG: Craig J. Goergen, 206 South Martin Jischke Drive, West Lafayette, Indiana, 47907, United States, Phone: (765) 494-1517, Fax: (765) 494-1193, cgoergen@purdue.edu.

Introduction

An abdominal aortic aneurysm (AAA) is a potentially life-threatening disease that accounts for approximately 11,000 deaths in the United States each year [1–3]. Aneurysms are caused by an initial insult to the aortic wall, leading to inflammatory cell infiltration, extracellular matrix remodeling, and vessel dilation [4]. Aortic dilation of 50% above normal diameter is considered aneurysmal and the only option for treatment is surgical intervention, by either open or endovascular repair [4]. Risk factors for AAAs include male gender, advanced age, smoking, hypertension, heritable predisposition, and atherosclerosis [1]. Noninvasive ultrasound is often used to detect and monitor aneurysm development [4–6]. Larger aneurysms have an increased risk of rupture, with 5 to 5.5 cm considered the typical threshold range for surgical intervention with slight variation depending on sex, country of treatment, and possible aneurysm shape. The rupture of an AAA is associated with 90% mortality and in many cases is the first and only clinical symptom of aortic expansion [4,7]. The fact that no medical therapies exist to limit aneurysm expansion indicates the need to better understand AAA pathophysiology.

Small animal models are often used to study AAAs as they mimic many aspects of the human disease [1,8]. Angiotensin II (AngII)-induced AAAs in apolipoprotein E-deficient (*apoE*$^{-/-}$) mice is one of the most common animal models used in the field [8]. The apoE gene is responsible for producing apolipoprotein E, a protein that combines with lipids in the body to form lipoproteins. The lipoproteins compartmentalize and transport cholesterol and fats through the bloodstream. Without the apoE gene (and protein), animals have higher circulating levels of cholesterol and eventually develop atherosclerosis [9]. When infused with AngII, *apoE*$^{-/-}$ mice become hypertensive and males are most likely to develop suprarenal dissecting AAAs with an incidence rate of roughly 60% [8,10]. While this mouse model has been used extensively due to the availability of *apoE*$^{-/-}$ and *LDLR*$^{-/-}$ transgenic mice [8,11–14], the combined effect of genetically induced hypercholesterolemia and chemically induced hypertension has not been explored in rats or other species. There are a number of advantages that a rat model can provide over mice when studying aortic aneurysms. For example, rats are physiologically, genetically, and morphologically closer to humans than mice [15–17]. The use of a larger rat model could also help develop biomedical devices and novel imaging techniques that are not possible in a smaller animal. For these reasons, we developed and characterized transgenic *apoE*$^{-/-}$ rats using transcription activator-like effector nucleases (TALENs).

The purpose of our study was to characterize the vascular pathology of *apoE*$^{-/-}$ rats with a specific focus on AAA development. We hypothesized that these rats would have increased serum cholesterol levels and when implanted with AngII-filled osmotic pumps would become hypertensive and develop suprarenal, dissecting AAAs.

Methods

Creation of apolipoprotein E-deficient rats

We generated *apoE*$^{-/-}$ rats using TALENs (Transposagen, Lexington KY) targeted to exon 4 of the rat apoE gene (third coding exon) located on chromosome 1. The nuclease recognition sequences used are as follows with the cut regions underlined:

5'-TGGGAGCTTCCAACTTTAAGAGCGAGCTTCGATTCGTCAGGAAGATGCTGTCA-3'

5'-TGTACAAGGCCGGGGCACAGGAGGGCGCCGAGCGCGGTGTGAGTGCTA-3'

Two pairs of circular DNA (10 ng/μl total DNA in 10 mM Tris-HCl, 0.1 mM EDTA) containing TALENs were microinjected simultaneously into the pronucleus of Hsd:Sprague Dawley fertilized eggs. We detected this mutation using a CEL1 mutation detection assay, which amplified heteroduplexed DNA (Integrated DNA technologies, Coralville IA) using the following primers:

5'-CCC TCT TGT GTT TCC TCT GG-3'

5'-TAT CTG CTG GGT CTG CTC CT-3'

The samples positive from the CEL1 assay were cloned with Taq polymerase and topoisomerase-charged vectors (TOPO TA Cloning Kit for Sequencing, Invitrogen, Carlsbad CA) and then sequenced to confirm a 16-basepair deletion in heterozygotes (S1 Fig).

We bred the founder male rat with a wildtype female and genotyped the tail clips from F2 progeny in order to identify animals homozygous for a 16-basepair deletion (AGGGCGCCGAGCGCGG; NCBI RefSeq Accession: NM_001270681.1). This sequence partially codes for a 22 amino acid approximate tandem repeat. When deleted, a frameshift mutation resulted (p.Glu178fs) upstream of a possible heparin-binding region according to sequence similarity with the human gene (UniProt Accession: P02650 and P02649) [18]. Immediately following the glutamate substitution, the protein is truncated by 134 amino acids.

To genotype the rats, we used PCR for DNA amplification (2.5 hour reaction cycle; 64.5 to 94°C) and purified the products (UltraClean PCR Clean-up Kit, MO BIO Laboratories, Carlsbad CA). We then used restriction enzyme digestion with NarI (New England BioLabs, Ipswich MA), a restriction endonuclease, which cuts after the second nucleotide of the sequence GGCGCC, generating cleavage products with 423- and 157-basepair bands in homozygotes compared to bands of 352-, 87-, and 157-basepairs in wild-types (S2 Fig).

We compared ApoE expression between wildtype and *apoE*$^{-/-}$ rats using harvested lung and spleen tissues (S3 Fig). ApoE is abundantly produced in these tissues (among others [19]). After euthanasia, 50 mg tissue samples were flash frozen with liquid nitrogen and stored at −80°C. Tissues were thawed on ice and resuspended in 800 ul lysis buffer (150 mM NaCl, 50 mM Tris-HCl pH 7.6, 1% TritonX-100, 0.1% SDS) supplemented with a protease

inhibitor cocktail (Roche, Indianapolis, IN) and 1.5 mM PMSF (Thermo Fisher Scientific, Waltham, MA). Soluble proteins were isolated by mechanical homogenization, incubation with mild agitation for 2 hours at 4°C, and centrifugation at 14,000 × g for 5 minutes. Samples for SDS-PAGE and Western Blot analysis were prepared by addition of 4X Laemmli sample buffer with a final concentration of 1% 2-mercaptoethanol (Sigma, St Louis, MO) and heated at 95°C for 10 min. Protein concentration was measured with the Pierce 660 nm Protein Assay with Ionic Detergent Compatibility Reagent (Thermo Fisher Scientific, Waltham, MA) and adjusted with 1X sample buffer to 2 mg/mL. A total of 60–80 μg total protein was loaded per lane and separated on a Mini-PROTEAN® TGX gradient (4–20%) gel (BioRad, Hercules, CA), followed by transfer to a PVDF membrane (BioRad, Hercules, CA). The membrane was blocked in Pierce Protein-free (TBS) blocking buffer (Thermo Fisher Scientific), then probed with an ApoE rabbit polyclonal antibody (ab20874, Abcam, Cambridge, MA; Antibody Registry ID AB_449883) diluted 1:1000 in 1:1 blocking buffer:Tris-buffered saline (TBS) with 0.05% Tween-20 (TBST) for approximately 3 hours at room temperature. The membrane was washed extensively in TBST, then probed with a polyclonal Cy5-conjugated goat anti-rabbit IgG (ab6564, Abcam; Antibody Registry ID AB_955061) diluted 1:10000 in 1:1 blocking buffer:TBST for approximately 2 hours at room temperature. The membrane was washed in TBST, then TBS, and the fluorescence was visualized using the Azure c400 (Azure Biosystems, Dublin, CA) (628/676, ex/em). To assure equal total protein loading, the membrane was stained with Ponceau red (Azure Biosystems, Dublin, CA) and imaged on an Epson V850Pro scanner. Precision Plus Protein Kaleidoscope Prestained Protein Standards (BioRad, Hercules, CA) were used to estimate the sizes of the protein bands (kDa).

Animal cohorts

The Purdue University Animal Care and Use Committee approved all animal experiments. Veterinary technicians maintained the rat cages and performed daily animal inspections. We used two cohorts of *apoE*$^{-/-}$ rats from our laboratory (Cohorts 1 and 3) and one cohort of commercially available *apoE*$^{-/-}$ Sprague-Dawley rats (Cohort 2) from Horizon Discovery (St. Louis MO). Horizon Discovery provided *apoE*$^{-/-}$ rats (TGRA3710; SD-ApoEtm1sage) with a 16-basepair deletion (within exon 3 on chromosome 1) with a confirmed loss of the ApoE protein [20]. All rats underwent surgery to implant mini-osmotic pumps filled with AngII (see below). We monitored the animals' appearance and well-being at 1, 24, and 48 hours post-surgery and provided post-operative care as necessary. Analgesics were not administered post-surgery due to the minimally invasive nature of the surgery. We followed each cohort for at least 28 days corresponding to the amount of time the mini-osmotic pumps elute AngII.

All rats were singly housed in contact bedding cages and fed a normal chow diet (Harlan Rodent Diet 2018, Indianapolis, IN) *ad libitum*. At the time of pump implantation surgery, animals in Cohort 1 (n=10; 8 males and 2 females) were 9 weeks old. Animals from Horizon Discovery were used for comparison (n=9 males) and were 9 weeks old at the time of surgery (Cohort 2). Rats in Cohort 3 (n=3 males) were implanted with pumps after reaching an older age (30 weeks).

Animals in Cohort 1a (n=5) are a subset of Cohort 1 and were sacrificed at 13 weeks of age. Rats in Cohort 1b represent a subset of Cohort 1 that was not sacrificed after the first study. These animals (n=5; 4 males and 1 female) were chosen randomly from the rats in Cohort 1. They were aged to 24 weeks at which point they were placed on an atherogenic diet containing 21.2% fat and 1.3% total cholesterol by weight (Harlan Rodent Diet TD.02028) *ad libitum* for the remainder of the study. At 30 weeks of age (the same age as animals in Cohort 3), these rats (n=4; 3 males and 1 female) had been consuming the new diet for 6 weeks. We then performed a second AngII pump implantation and followed these animals for 4 weeks before sacrifice (n=3; 2 males and 1 female).

We followed Horizon Discovery rats (Cohort 2) as two groups. Animals in Cohort 2a (n=3) were followed for 4 weeks and sacrificed at 13 weeks of age (the same end point as Cohort 1a). Rats in Cohort 2b (n=6) are a second subset that we began following at the same age as Cohort 2a but these animals were exposed to AngII for a prolonged period of time (8 weeks). We implanted a second pump in each rat at 13 weeks of age and sacrificed at 18 weeks of age. Figure 1 details the timeline for the pump implantation surgeries, blood pressure measurements, high-fat diet administration, blood collection, and sacrifice endpoints.

Osmotic pump implantation

We implanted an AngII mini-osmotic pump (ALZET Model 2004; DURECT Corporation, Cupertino CA) subcutaneously in the left dorsum of each rat. AngII powder (MW: 1046.19; Bachem, Torrance CA) was first solubilized in sterile 0.9% saline and loaded into the pumps according to animal weight (200 ng/kg/min infusion rate [21] for 28-day duration). To prime the pumps, we incubated them in sterile saline at 37°C overnight before implantation. We performed the same procedure to implant a second pump in the rats in Cohorts 1b and 2b. The first expired pump remained in the rat and the new pump was placed on the opposite side of the animal. No *apoE*$^{-/-}$ rats were implanted with saline-filled pumps to serve as a control.

Cholesterol analysis and *en face* aortic staining

A blood serum cholesterol assay (Bioassay Kit Metabolism, Fisher Scientific Co.) was used to analyze total cholesterol in Cohorts 1b, 2, and 3. Tail vein blood (>60 μL) was collected approximately one week prior to pump implantation. Additionally, once Cohort 1b had begun consuming a high fat diet, blood samples were taken 2, 5, and 6 weeks after the start of the new diet. Samples were centrifuged (7,800 × g, 5 minutes) to collect serum, which was stored at 4°C until analysis. A full lipid panel consisting of cholesterol, triglycerides, high-density lipoproteins (HDL), and low-density lipoproteins (LDL) was also conducted (IDEXX Bioresearch, North Grafton, MA) on serum samples from wildtype (n=3; 93.7±7.4 days of age) and *apoE*$^{-/-}$ (n=3; 40±0 days of age) rats.

Furthermore, we examined the intimal surface of rat aortas *ex vivo* for the presence of lipid-rich plaques. We removed the periadventitial fat and connective tissue from aortas and cut them longitudinally to expose the inner luminal surface. We acquired high-magnification

images of the aortic tree before and after staining with 0.5% Sudan IV solution (Sigma, St Louis MO).

Blood pressure

We noninvasively measured the blood pressure of conscious rats using a tail cuff system [22] specifically designed for small animals (2 Channel CODA System, Kent Scientific Corp., Torrington CT). Systolic, diastolic, and mean arterial blood pressures were recorded one week before pump implantation, three days after implantation, and once a week during a 28-day study period. At each time point, we acquired between 40 and 60 runs using an occlusion pressure of 250 mmHg and a deflation time of 15 to 20 seconds.

Small animal ultrasound

We performed *in vivo* ultrasonography (US) of all *apoE*$^{-/-}$ rats with a high-resolution, small animal US system (Vevo2100 Imaging System; FUJIFILM VisualSonics, Toronto, ON Canada). We acquired transaxial and longitudinal US images prior to surgeries (day 0) and at days 3, 7, 14, 21, and 28 post-surgery using a 256-element, linear array transducer (MS250D, 13–24 MHz, 21 MHz center frequency). For Cohort 2b, we also acquired US data on day 56 (or 28 days after the second pump implantation).

The rats were initially anesthetized with isoflurane (2–4% in 1 L/min medical grade air) and then kept unconscious during imaging with isoflurane at 1–2.5%. Prior to imaging, animals were positioned supine on an adjustable heated stage, sterile eye lubricant was applied to each eye, and hair was removed on the ventral abdominal region with depilatory cream. We noninvasively monitored heart and respiration rate through stage electrodes and body temperature using a rectal probe. The animals were kept at approximately 37°C throughout the imaging procedure. The transducer was positioned perpendicular to the animal and held stable with a rail mount system. US gel (Aquasonic 100; Parker Laboratories; Fairfield, NJ) was applied to create an acoustic impedance-matching layer between the transducer and the animal's skin. We adjusted the angle of the stage as necessary to optimize visualization of the aorta in the long- and short-axis. We identified anatomical landmarks (such as the inferior vena cava, renal veins, and aortic bifurcation) for orientation, and observed the presence of pulsatile vessel motion to help distinguish arteries from veins.

During each session of imaging, high-resolution 2D images were acquired of the suprarenal abdominal aortic region of each rat using brightness mode (B-mode; 300 frames), motion mode (M-mode; five-second acquisition), pulsed wave (PW) and color Doppler (five-second acquisitions) modes. We adjusted the transducer beam angle and PW Doppler angle (30–60 degrees from vertical) in order to accurately detect the velocity and direction of blood flow.

We used VisualSonics VevoLab software to analyze the imaging datasets. B-mode data acquired in long-axis was analyzed to determine mean aortic diameter. We traced aortic specular reflections, representing the inner diameter of the vessel, on M-mode images in order to calculate circumferential Green-Lagrange cyclic strain. For a given M-mode acquisition, we chose two reflective lines, one along the anterior and one along the posterior vessel wall. We chose lines that could be tracked over multiple cardiac cycles so that we could make multiple inner diameter measurements over time. We made a point of not

making measurements when the animal was inhaling because the aorta undergoes significant motion.

We also acquired respiration- and cardiac-gated transaxial US volumes of the suprarenal aorta beginning inferior to the renal arteries and up to the diaphragm (3 cm total scan distance; 0.19 mm step size). Lastly, automatic frequency tracing over the peaks of PW Doppler velocity waveforms was used in order to measure mean blood flow velocity over a cardiac cycle.

Tissue collection

Rats were euthanized as indicated in Figure 1 (at the point where the line ends in each row). Rats used for histology (Cohorts 2a and 3) were pressure perfused through the left ventricle, as described previously [23]. We excised the heart and aorta and allowed them to fix in 4% paraformaldehyde for 24 hours. Tissue was kept in phosphate-buffered saline until gross vessel dissection. We also collected the suprarenal aortas from four wildtype Sprague-Dawley rats (17±7.6 weeks of age and 378±83.2 g at sacrifice) for measurements of the cross-sectional area of the media.

Aortic tissue histology

We segmented suprarenal and ascending aortas prior to paraffin embedding, sectioning (5 μm), and staining (H&E, Verhoeff Van-Gieson (VVG), and Masson's Trichrome (MTC)). VVG and MTC stains were used to distinguish elastin bands (black) and collagen fibers (blue), respectively, from adjacent structures. We scanned images (4X and 10X magnification) for qualitative and quantitative analysis. For the latter, we measured the cross-sectional area of the media (between the inner and outer elastic layers) of each VVG-stained suprarenal aorta tissue section (ImageJ; [24]). Additionally, we examined ascending aortas from *apoE*$^{-/-}$ (n=3; 442±66 days of age) and wildtype (n=3; 102±28 days of age) rats that were fed regular chow and not infused with AngII. This location is the site for early development of atherosclerotic lesions and thoracic aortic aneurysms in mice [25,26].

Statistical analysis

Data values are presented as mean ± standard deviation. We performed parametric and non-parametric tests to analyze statistical differences for Cohorts 1, 2, and 3 as well as wildtype rats at different time points. We used one-way analysis of variance (ANOVA) with post-hoc tests (Dunnett's and Tukey HSD) to analyze serially collected blood pressure and total serum cholesterol data. We ran two-tailed Student's t-tests (unpaired and paired) to compare US-derived measurements, serum lipid levels, and values for the cross-sectional area of the aortic media. Additionally, we used Kruskal-Wallis test followed by Dunn's multiple comparisons to analyze US-derived measurements for Cohort 2 and to compare across cohorts at a single time point. A p-value of 0.05 or lower was considered significant. We performed power analysis for the expected change in aortic diameter for rats developing AAAs post-surgery. Based on the current clinical diagnostic threshold of 50% increase, we calculated that a sample size of 4 would be required to attain statistical power of at least 0.8 at an alpha of 0.05.

Results

Body weight gain and animal mortality

At the time of pump implantation for Cohort 1 (9 weeks of age), the average weight of male rats (n=8) was 315±12.9 g and the two female rats weighed 217 and 224 g (S4 Fig). Animals from Horizon Discovery (n=9) had a similar weight (319±7.8 g) at 9 weeks of age when pumps were implanted (S4 Fig). At 28 weeks of age, animals in Cohort 3 (n=3) weighed 493±40.2 g. At the same age, the male rats (n=3) and one female rat in Cohort 1b weighed 497±5.0 and 319 g, respectively. After the start of the HFD, animals in Cohort 1b did not experience an increase in weight (S4 Fig). Two animals in Cohort 1b (one male and one female) died 5–7 weeks after the start of the HFD. One male animal in Cohort 2b also died after 6 weeks of AngII infusion. Details on these premature deaths are provided below.

Total serum cholesterol measurements and *en face* staining

We compared total serum cholesterol values from Cohorts 1b, 2, and 3 in order to measure the degree of dyslipidemia in this model (Table 1 and S1 Table). 20-week-old chow-fed rats (Cohort 1b) showed significantly higher serum cholesterol as compared to wildtype animals (190.5±13.4 vs. 104.7±14.2 mg/dL; $p<0.01$). Cohort 1b also had statistically significant elevations in serum cholesterol levels over 6 weeks of HFD (236.6±8.9 – 267.5±10.3 mg/dL) relative to baseline and time points during the HFD ($p<0.05$) except at one intermediate time point. We observed substantial visceral fat during dissection of the two animals that died after 5–7 weeks on the HFD, suggesting that death might have been due to complications with the diet as observed by others [27–29]. Cohort 3 also had significantly higher serum cholesterol at 8 and 28 weeks of age (136.1±5.5 – 147.7±8.4 mg/dL) as compared to wildtype animals ($p<0.05$). These values were similar to those measured in two rats at 9 weeks of age in Cohort 2 (145.1 and 127.1 mg/dL; S1 Table), but lower than those for Cohort 1b. Full serum analysis of a subset of rats further confirmed a significant shift between serum cholesterol values for wildtype and $apoE^{-/-}$ rats (S5 Fig and S1 Table). Cholesterol and LDL were significantly elevated (6.9±2.5- and 10.7±3.2-fold) while HDL had a borderline significant reduction (0.5±0.2-fold) in $apoE^{-/-}$ rats. LDL/HDL ratio was also significantly increased (20.8±8.7-fold) for the $apoE^{-/-}$ rats. Taken together, our results demonstrate that $apoE^{-/-}$ rats have elevated total serum cholesterol and that these levels are sensitive to HFD. None of the aortas prepared *en face* showed appreciable atherosclerosis as determined by minimal accumulation of Sudan IV stain on the luminal surface (S6 Fig).

Elevation in blood pressure with angiotensin II infusion

Systolic, diastolic, and mean arterial blood pressure increased in all rats after implantation of pumps (S1 Table). As early as day 3 post-implantation we measured increases in these values and at day 14 these values began to plateau. In Fig 2, we have displayed systolic blood pressure (SBP) values as a function of animal age rather than days post-implantation. As compared to Cohort 1, baseline SBP values were higher for age-matched Horizon Discovery animals in Cohort 2 ($p=0.043$) and the older animals in Cohort 3 ($p=0.035$). The elevation in SBP was statistically significant from baseline by day 14 for Cohorts 1 and 3 (Fig 2A) and by day 3 for Cohort 2 (Fig 2B). The largest percent increases were 60±20% (Cohort 1), 40±5% (Cohort 2), and 30±4% (Cohort 3). For animals in Cohort 1b, the largest

percent increase relative to levels just prior to re-implantation was 29±5%. Animals continuously infused with AngII for more than four weeks (Cohort 2b) had a statistically significant elevation in SBP that was sustained for 56 days (Fig 2B). SBP was increased 50±4% relative to baseline by day 21 after re-implantation. One male rat in Cohort 2b died after 6 weeks of AngII infusion. This animal experienced weight loss that could not be alleviated by saline injections. On necropsy we found that it may have had an abdominal perforation leading to internal bleeding. We also found that Sprague-Dawley wildtype rats (n=10) not infused with AngII have similar blood pressures as *apoE*$^{-/-}$ rats prior to pump implantation (S1 Table). The rats in the present study, therefore, show baseline blood pressure values that are similar to wildtype controls and moderate to severe hypertension in response to AngII.

Ultrasound measurements

We observed no aortic dissections or AAAs over 28 and 56 days of AngII infusion. Across cohorts, suprarenal aortic diameter ranged between 1.70 and 2.61 mm at baseline to 1.65 and 2.98 mm at day 28 (Fig 3). Older rats (Cohorts 1b and 3) had similar values over 28 days (p=0.45 and p=0.18, respectively). The aortas of younger rats (Cohorts 1 and 2) showed a small increase in diameter over 28 days (p=0.046 and p=0.054, respectively), which we attribute primarily to growth of the animals as they aged between weeks 9 and 13. Over this period, two animals in Cohort 1 experienced the largest change in diameter (38 and 70% increase) among all animals. Animals in Cohort 2b had a statistically significant increase in aortic diameter after 56 days of AngII infusion (p<0.001). The largest individual percent increase in diameter over this period was 51%, but no focal enlargement was observed. Despite similar ages, baseline aortic diameter for Cohort 2 as compared to Cohort 1 was significantly larger (29±3%; p<0.001). A three-dimensional rendering of segmentations from the suprarenal aorta of a rat from Cohort 3 is shown in the S1 Movie. The overall morphology and size of this aorta remained relatively normal after 28 days of AngII infusion.

We found that animals in Cohorts 1, 2, and 3 had variable changes in mean blood flow velocity through the suprarenal aorta at day 28 relative to baseline (Fig 4). Averaging these changes for the animals in each cohort, we measured small reductions in blood flow velocity. The two animals in Cohort 1 with the largest change in aortic diameter also had the largest decrease in mean blood flow velocity (44 and 45% decrease). The three animals in Cohort 3 experienced a 14±2% increase in diameter alongside a statistically significant 33±12% decrease in mean blood flow velocity.

Circumferential cyclic strain was significantly reduced at days 28 and 56 relative to baseline except Cohort 1b (Fig 5). Comparing Cohort 3 (normal diet) with Cohort 1b (HFD), there was no significant difference in circumferential cyclic strain at days 0 (p=0.051) or 28 (p=0.174). As animals in Cohort 1b were implanted with a second pump after the first one had expired, we also analyzed the effect of repeat AngII infusion after a 17-week interruption. After this period of time when no exogenous AngII was being delivered (between 13 and 30 weeks of age), blood pressure (Fig 2A) and circumferential cyclic strain (Fig 5A) values for these animals shifted towards baseline values while the diameter

increased slightly. Animals in Cohort 2 had a statistically significant reduction in circumferential cyclic strain after 28 days of AngII infusion ($p<0.001$). This magnitude of reduction for the animals in Cohort 2b was similar after the second AngII infusion period (i.e. day 56). The two animals with the largest increase in aortic diameter also had the greatest reduction in circumferential cyclic strain (40 and 80% decrease).

Histology

Suprarenal aortas exhibited healthy elastin and collagen structure (S7 Fig A and B), confirming our *in vivo* observations that the aortic morphology remained mostly normal after 28 days of AngII infusion. We did however find that the medial layer became significantly larger ($p=0.0036$) in rats infused with AngII as compared to those without AngII infusion (Fig 6A and B). Mean cross-sectional area of the media was 1.6-fold greater for the AngII-infused group (0.70 ± 0.12 mm^2; n=8) as compared to those without infusion (0.44 ± 0.1 mm^2; n=4; Fig 6C). There was no statistically significant difference in the ages or weights of the animals between these groups. We also noted large nuclei in the aortic smooth muscle cells of rats infused with AngII (Fig 6A, H&E). We observed no atherosclerotic plaques and healthy elastic lamellar units in the ascending aortas of older *apoE*$^{-/-}$ rats not infused with AngII (S7 Fig C).

Discussion

Our studies demonstrate that *apoE*$^{-/-}$ rats develop a moderate cardiovascular disease phenotype but do not develop dissecting AAAs when infused with AngII. Our findings suggest that there are species-specific differences between mice and rats that in response to ApoE-deficiency and atherosclerosis susceptibility may explain why we did not observe AAA formation.

Species-specific differences between rats and mice

Rats have several physiological and morphological differences when compared to mice. Interestingly, however, the aorta of both species exhibits a leftward curvature above the right renal artery, which has been proposed as a determining factor for leftward expansion of AngII AAAs in mice [30,31]. *In vivo* circumferential cyclic strain is also similar across rats and mice, suggesting there is similar pulsatile loading of the aorta [32]. Despite these factors, AAAs did not develop in *apoE*$^{-/-}$ rats infused with AngII. In light of the findings described here, there are three areas that could be explored further to understand AAA formation and development.

First, future work could focus on quantifying how blood flow and hemodynamic metrics, such as wall shear stress and oscillatory shear index [33,34], evolve between a healthy and diseased state. This can be accomplished by computational fluid dynamic modeling to investigate how regional differences in flow patterns influence vascular growth and remodeling of the aorta [35,36]. We have previously shown how biomechanical and hemodynamic factors are influenced after AngII AAA formation in mice [23]. However, the role that hemodynamics [4,37,38] and biomechanics [39,40] play as an initiating factor for the disease requires further investigation in animal models and humans.

Second, serum lipids and lipoproteins may impact cardiovascular disease development differently in *apoE*$^{-/-}$ mice and rats. Hyperlipidemic mice have a significantly larger fraction of non-high-density lipoproteins than wildtype mice [41]. A shift towards increased levels of total cholesterol and decreased levels of HDL is an important factor for atherogenesis and may influence AngII AAA development [42]. Wei et al. recently reported that rats with a 14-basepair apoE gene deletion had a LDL/HDL ratio in the serum of greater than 4:1 after consuming a HFD for 12 weeks [43]. They concluded that their rats do not spontaneously become hyperlipidemic and that a HFD and partial carotid ligation are necessary to promote atherogenesis. Therefore, further characterization of atherosclerosis in *apoE*$^{-/-}$ rats is certainly justified. In the present work, we found that chow-fed *apoE*$^{-/-}$ rats have significantly higher serum cholesterol, LDL, and LDL/HDL than wildtype rats and that a HFD exacerbated the elevation in total serum cholesterol but did not lead to atherosclerosis. Future work would be needed to determine if a different HFD is necessary to shift the lipoprotein profile further towards a pro-atherogenic state. In agreement with other findings from Wei et al. [43], aortas in our study showed no lipid accumulation or visible plaque on the luminal surface (S6 and S7 Figs). Taken together, these data suggest that the lack of atherosclerosis in *apoE*$^{-/-}$ rats may play a role in the absence of AAA formation. However, development of atherosclerotic lesions at the level of the suprarenal aorta has been shown to not be necessary for AAA development [44]. Third, a heightened response to AngII in rats as compared to mice entails several differences in physiology and vascular remodeling [21], as further described below.

Effect of angiotensin II on physiology and vascular remodeling

The animals in this study became hypertensive relative to baseline levels (Fig 2) over 28 days of subcutaneous infusion of exogenous AngII (200 ng/kg/min). We chose this dose based on previous studies in wildtype rats [21,45–47]. Cassis et al. previously showed that higher doses of AngII had detrimental physiological effects including loss in body weight [46]. At a dose of 200 ng/kg/min, animals in our study maintained their body weight while blood pressure increases were consistent with those in previous work [21,45,46], confirming that the pumps eluted AngII properly. Past studies have also verified that saline-filled pumps implanted in rats do not cause a rise in blood pressure [21,46]. Based on this work and our current findings with consistent baseline measurements, we did not implant *apoE*$^{-/-}$ rats with saline-filled pumps.

It is clear that AngII infusion promotes atherogenesis and it is required for formation of AAAs in hyperlipidemic or wildtype mice [44,48,49]. In *apoE*$^{-/-}$ rats, however, it is not yet clear whether an optimized dosage of exogenous AngII would be sufficient to cause atherosclerosis and AAAs. Cassis et al. extensively characterized how much less responsive C57BL/6 mice are to AngII than Sprague-Dawley rats [21]. One noteworthy difference between species is evidence of medial hypertrophy and thickening in rats, but adventitial expansion in mice in response to AngII infusion [21]. Our images and quantification of medial layer thickening in the present study confirm this finding in *apoE*$^{-/-}$ rats infused with AngII as compared to both the suprarenal aortas of rats not infused with AngII (Fig 6) and previously published data for the thoracic [50,51] and infrarenal [52] aorta. Findings from other studies may also support this. Su et al. provided evidence of proliferation of smooth

muscle cells in smaller rat arteries as a result of AngII infusion [53]. Cao et al. have also shown that AngII infusion in rats is associated with a significant increase in the density of AngII binding sites on the cells in vessel walls [54]. Cassis et al. reiterated this finding in their comparative animal study and concluded that unlike in rats, there is "downregulation of AngII receptor density in mouse tissues following chronic AngII infusion" [21]. This may partly explain why a more hypertensive response is seen in rats compared to mice for the same dosage of exogenous AngII.

Serum cholesterol levels

In planning our experiments, we decided to use standard chow, as Horizon Discovery described adverse effects and death in *apoE*$^{-/-}$ rats fed a HFD [20]. For Cohort 1b, however, we chose to place this subset of animals on a HFD with the goal of increasing their atherogenic potential. These rats did not show a change in weight after the start of the HFD (S4 Fig). We cannot verify however that these animals had low food intake, as we did not track this. Horizon Discovery has provided unpublished total serum cholesterol values for *apoE*$^{-/-}$ rats [20]. These levels are two- to three-fold higher as compared to those for our age-matched rats (Cohorts 1b and 3) when consuming standard chow. This discrepancy may be due to the use of different assay kits. Cholesterol levels were similar between the *apoE*$^{-/-}$ rats we created and those bought commercially (Table 1 and S1 Table). This indicates that our cholesterol assay is indeed detecting comparable values for total serum cholesterol in each knockout model. Additionally, levels in age-matched wildtype rats were significantly lower. Future experiments could investigate other atherogenic diets and serum cholesterol levels using a fluorimetric assay.

Ultrasound imaging

From our analysis of US data and inspection of the gross morphology and cross-sectional histology of the aortas, we confirmed that no AAAs developed. However, suprarenal aortic diameter and mean blood flow velocity did have some statistically significant differences over time (Figs 3 and 4). A study from 2003 that used lower-frequency US to track experimental AAAs concluded that normal weight gain and aortic growth in rats could confound one's ability to determine aortic expansion over periods longer than 14 days [55]. Natural growth should certainly be considered in analyzing serial measurements. That being said, high-frequency US provides high resolution that is adequate to identify pathological expansion. In mice, AngII-induced AAAs are focal and saccular [8,23], which make them easy to distinguish from a healthy aorta. We did find that circumferential cyclic strain of the suprarenal aorta was reduced relative to baseline for all cohorts (Fig 5). These changes are likely due to the hypertension that occurred after AngII pump implantation, moving vessel loading up the stress-strain curve. Due to this increased load, more collagen may be deposited and remodeled, causing the aorta to become less compliant.

Summary

We have characterized the vascular pathology in young and old Sprague-Dawley rats with ApoE deficiency. The animals showed an increase in total serum cholesterol levels, particularly with HFD feeding, and a rise in blood pressure after implantation of AngII

miniosmotic pumps. We also found that animals had decreased suprarenal circumferential cyclic strain and larger medial layers, which we attribute to hypertension and arterial wall remodeling. Suprarenal aortas had preserved elastin and collagen structure after 28 days of infusion but the cross-sectional area of the media became larger. However, we did not observe aortic dissection or focal enlargement of the suprarenal aorta, as has been observed in AngII-infused *apoE*$^{-/-}$ mice. Furthermore, we did not identify atherosclerotic plaques or lipid accumulation on the luminal surface of aortas. Overall these findings suggest that *apoE*$^{-/-}$ rats have a moderate cardiovascular disease phenotype that is resistant to atherosclerosis and AAA formation despite HFD administration and exogenous AngII infusion. Atherosclerosis may be a crucial initiating factor for AngII-induced AAAs and we suspect there are several species-specific differences that explain why we see resistance to cardiovascular disease in rats. Future work will be needed to use our US data for computational fluid dynamic modeling and to analyze the presence of specific inflammatory cells in the aortic wall. In comparison to mice, a rat model has potential utility to help with translational studies involving biomedical devices, imaging, and experimental therapeutics.

Supplementary Material

Refer to Web version on PubMed Central for supplementary material.

Acknowledgments

We gratefully acknowledge Rebecca Houser and Judy Hallett in the Transgenic Mouse Facility at Purdue University for their help creating and genotyping the transgenic rats. We also acknowledge the assistance of the Purdue University Histology Research Laboratory, a core facility of the NIH-funded Indiana Clinical and Translational Science Institute.

Acknowledgment of support: Funding was provided by an American Heart Association Scientist Development Grant (14SDG18220010) and the Indiana Clinical and Translational Sciences Institute, in part by Grant Number (UL1TR001108) from the National Institutes of Health, National Center for Advancing Translational Sciences, Clinical and Translational Sciences Award to CJG. The content is solely the responsibility of the authors and does not necessarily represent the official views of the National Institutes of Health.

References

1. Brady AR, Thompson SG, Fowkes FGR, Greenhalgh RM, Powell JT. UK Small Aneurysm Trial Participants. Abdominal aortic aneurysm expansion: risk factors and time intervals for surveillance. Circulation. 2004 Jul 6.110:16–21. [PubMed: 15210603]
2. Hirsch AT, Haskal ZJ, Hertzer NR, Bakal CW, Creager MA, Halperin JL, et al. ACC/AHA 2005 Practice Guidelines for the management of patients with peripheral arterial disease (lower extremity, renal, mesenteric, and abdominal aortic): a collaborative report from the American Association for Vascular Surgery/Society for Vascular Surgery, Society for Cardiovascular Angiography and Interventions, Society for Vascular Medicine and Biology, Society of Interventional Radiology, and the ACC/AHA Task Force on Practice Guidelines (Writing Committee to Develop Guidelines for the Management of Patients With Peripheral Arterial Disease): endorsed by the American Association of Cardiovascular and Pulmonary Rehabilitation; National Heart, Lung, and Blood Institute; Society for Vascular Nursing; TransAtlantic Inter-Society Consensus; and Vascular Disease Foundation. Circulation. 2006 Mar 21.113:e463–654. [PubMed: 16549646]
3. Go AS, Mozaffarian D, Roger VL, Benjamin EJ, Berry JD, Borden WB, et al. Heart disease and stroke statistics--2013 update: a report from the American Heart Association. Circulation. 2013 Jan 1.127:e6–e245. [PubMed: 23239837]
4. Dalman RL, Tedesco MM, Myers J, Taylor CA. AAA disease: mechanism, stratification, and treatment. Ann N Y Acad Sci. 2006 Nov.1085:92–109. [PubMed: 17182926]

5. d'Audiffret A, Desgranges P, Kobeiter DH, Becquemin JP. Follow-up evaluation of endoluminally treated abdominal aortic aneurysms with duplex ultrasonography: validation with computed tomography. J Vasc Surg. 2001 Jan.33:42–50. [PubMed: 11137922]
6. AbuRahma AF, Welch CA, Mullins BB, Dyer B. Computed tomography versus color duplex ultrasound for surveillance of abdominal aortic stent-grafts. J Endovasc Ther. 2005 Oct.12:568–573. [PubMed: 16212456]
7. Powell JT, Greenhalgh RM. Clinical practice. Small abdominal aortic aneurysms. N Engl J Med. 2003 May 8.348:1895–1901. [PubMed: 12736283]
8. Daugherty A, Manning MW, Cassis LA. Angiotensin II promotes atherosclerotic lesions and aneurysms in apolipoprotein E-deficient mice. J Clin Invest. 2000 Jun.105:1605–1612. [PubMed: 10841519]
9. Moghadasian MH, McManus BM, Nguyen LB, Shefer S, Nadji M, Godin DV, et al. Pathophysiology of apolipoprotein E deficiency in mice: relevance to apo E-related disorders in humans. FASEB J. 2001 Dec.15:2623–2630. [PubMed: 11726538]
10. Trachet B, Fraga-Silva RA, Jacquet PA, Stergiopulos N, Segers P. Incidence, severity, mortality, and confounding factors for dissecting AAA detection in angiotensin II-infused mice: a meta-analysis. Cardiovasc Res. 2015 Aug 24.doi: 10.1093/cvr/cvv215
11. Daugherty A, Cassis L. Chronic angiotensin II infusion promotes atherogenesis in low density lipoprotein receptor −/− mice. Ann N Y Acad Sci. 1999 Nov 18.892:108–118. [PubMed: 10842656]
12. Usui F, Shirasuna K, Kimura H, Tatsumi K, Kawashima A, Karasawa T, et al. Inflammasome Activation by Mitochondrial Oxidative Stress in Macrophages Leads to the Development of Angiotensin II-Induced Aortic Aneurysm. Arterioscler Thromb Vasc Biol. 2014 Nov 6.35:127–136. [PubMed: 25378412]
13. Cassis LA, Rateri DL, Lu H, Daugherty A. Bone marrow transplantation reveals that recipient AT1a receptors are required to initiate angiotensin II-induced atherosclerosis and aneurysms. Arterioscler Thromb Vasc Biol. 2007 Feb.27:380–386. [PubMed: 17158350]
14. Schriefl AJ, Collins MJ, Pierce DM, Holzapfel GA, Niklason LE, Humphrey JD. Remodeling of intramural thrombus and collagen in an Ang-II infusion ApoE−/− model of dissecting aortic aneurysms. Thromb Res. 2012 Sep.130:e139–46. [PubMed: 22560850]
15. Gibbs RA, Weinstock GM, Metzker ML, Muzny DM, Sodergren EJ, Scherer S, et al. Genome sequence of the Brown Norway rat yields insights into mammalian evolution. Nature. 2004 Apr 1.428:493–521. [PubMed: 15057822]
16. Jacob HJ, Kwitek AE. Rat genetics: attaching physiology and pharmacology to the genome. Nature Reviews Genetics. 2002 Jan.3:33–42.
17. Lin JH. Species similarities and differences in pharmacokinetics. Drug Metab Dispos. 1995 Oct. 23:1008–1021. [PubMed: 8654187]
18. The UniProt Consortium. UniProt: a hub for protein information. Nucleic Acids Res. 2015 Jan 15.43:D204–D212. [PubMed: 25348405]
19. [cited 2017 Jan 26] Anti-Apolipoprotein E antibody (ab20874) [Internet]. Abcam. Available from: http://www.abcam.com/apolipoprotein-e-antibodyab20874.html
20. [cited 2016 Mar 14] Horizon Discovery - In Vivo Models - ApoE Knockout Rat [Internet]. Horizon Discovery. Available from: https://www.horizondiscovery.com/apoe-knockout-rat-tgra3710
21. Cassis LA, Huang J, Gong MC, Daugherty A. Role of metabolism and receptor responsiveness in the attenuated responses to Angiotensin II in mice compared to rats. Regul Pept. 2004 Feb 15.117:107–116. [PubMed: 14700746]
22. Feng M, Whitesall S, Zhang Y, Beibel M, D'Alecy L, DiPetrillo K. Validation of volume-pressure recording tail-cuff blood pressure measurements. Am J Hypertens. 2008 Dec.21:1288–1291. [PubMed: 18846043]
23. Phillips EH, Yrineo AA, Schroeder HD, Wilson KE, Cheng J-X, Goergen CJ. Morphological and Biomechanical Differences in the Elastase and AngII apoE−/− Rodent Models of Abdominal Aortic Aneurysms. Biomed Res Int. 2015 May 4.2015:12.
24. Rasband, SW., editor. [cited 2016 Jun 20] ImageJ [Internet]. U. S. National Institutes of Health. 1997. Available from: http://imagej.nih.gov/ij/

25. Rateri DL, Davis FM, Balakrishnan A, Howatt DA, moorleghen JJ, O'Connor WN, et al. Angiotensin II induces region-specific medial disruption during evolution of ascending aortic aneurysms. Am J Pathol. 2014 Sep.184:2586–2595. [PubMed: 25038458]
26. Trachet B, Piersigilli A, Fraga-Silva RA, Aslanidou L, Sordet-Dessimoz J, Astolfo A, et al. Ascending Aortic Aneurysm in Angiotensin II-Infused Mice: Formation, Progression, and the Role of Focal Dissections. Arterioscler Thromb Vasc Biol. 2016 Apr.36:673–681. [PubMed: 26891740]
27. Lichtman AH, Clinton SK, Iiyama K, Connelly PW, Libby P, Cybulsky MI. Hyperlipidemia and atherosclerotic lesion development in LDL receptor-deficient mice fed defined semipurified diets with and without cholate. Arterioscler Thromb Vasc Biol. 1999 Aug.19:1938–1944. [PubMed: 10446074]
28. Vergnes L, Phan J, Strauss M, Tafuri S, Reue K. Cholesterol and cholate components of an atherogenic diet induce distinct stages of hepatic inflammatory gene expression. J Biol Chem. 2003 Oct 31.278:42774–42784. [PubMed: 12923166]
29. Samokhin AO, Wilson S, Nho B, Lizame MLG, Musenden OEE, Bromme D. Cholatecontaining high-fat diet induces the formation of multinucleated giant cells in atherosclerotic plaques of apolipoprotein E−/− mice. Arterioscler Thromb Vasc Biol. 2010 Jun.30:1166–1173. [PubMed: 20203298]
30. Goergen CJ, Azuma J, Barr KN, Magdefessel L, Kallop DY, Gogineni A, et al. Influences of Aortic Motion and Curvature on Vessel Expansion in Murine Experimental Aneurysms. Arterioscler Thromb Vasc Biol. 2011 Feb.31:270–279. [PubMed: 21071686]
31. Goergen CJ, Barr KN, Huynh DT, Eastham-Anderson JR, Choi G, Hedehus M, et al. In vivo quantification of murine aortic cyclic strain, motion, and curvature: implications for abdominal aortic aneurysm growth. J Magn Reson Imaging. 2010 Oct.32:847–858. [PubMed: 20882615]
32. Goergen CJ, Johnson BL, Greve JM, Taylor CA, Zarins CK. Increased anterior abdominal aortic wall motion: possible role in aneurysm pathogenesis and design of endovascular devices. J Endovasc Ther. 2007 Aug.14:574–584. [PubMed: 17696635]
33. Trachet B, Renard M, Santis G, Staelens S, Backer J, Antiga L, et al. An Integrated Framework to Quantitatively Link Mouse-Specific Hemodynamics to Aneurysm Formation in Angiotensin II-infused ApoE−/− mice. Ann Biomed Eng. 2011 May 26.39:2430–2444. [PubMed: 21614649]
34. Greve JM, Les AS, Tang BT, Draney Blomme MT, Wilson NM, Dalman RL, et al. Allometric scaling of wall shear stress from mice to humans: quantification using cine phase-contrast MRI and computational fluid dynamics. Am J Physiol Heart Circ Physiol. 2006 Oct.291:H1700–8. [PubMed: 16714362]
35. Les AS, Shadden SC, Figueroa CA, Park JM, Tedesco MM, Herfkens RJ, et al. Quantification of hemodynamics in abdominal aortic aneurysms during rest and exercise using magnetic resonance imaging and computational fluid dynamics. Ann Biomed Eng. 2010 Apr.38:1288–1313. [PubMed: 20143263]
36. Di Achille P, Tellides G, Figueroa CA, Humphrey JD. A haemodynamic predictor of intraluminal thrombus formation in abdominal aortic aneurysms. Proceedings of the Royal Society A: Mathematical, Physical and Engineering Sciences. 2014 Oct 8.470:20140163–20140163.
37. Amirbekian S, Long RC, Consolini MA, Suo J, Willett NJ, Fielden SW, et al. In vivo assessment of blood flow patterns in abdominal aorta of mice with MRI: implications for AAA localization. Am J Physiol Heart Circ Physiol. 2009 Oct.297:H1290–5. [PubMed: 19684182]
38. Ford MD, Black AT, Cao RY, Funk CD, Piomelli U. Hemodynamics of the mouse abdominal aortic aneurysm. J Biomech Eng. 2011 Dec.133:121008. [PubMed: 22206425]
39. Danpinid A, Luo J, Vappou J, Terdtoon P, Konofagou EE. In vivo characterization of the aortic wall stress-strain relationship. Ultrasonics. 2010 Jun.50:654–665. [PubMed: 20138640]
40. Collins MJ, Bersi M, Wilson E, Humphrey JD. Mechanical properties of suprarenal and infrarenal abdominal aorta: implications for mouse models of aneurysms. Med Eng Phys. 2011 Dec. 33:1262–1269. [PubMed: 21742539]
41. Zhang SH, Reddick RL, Piedrahita JA, Maeda N. Spontaneous hypercholesterolemia and arterial lesions in mice lacking apolipoprotein E. Science. 1992 Oct 16.258:468–471. [PubMed: 1411543]

42. Prins PA, Hill MF, Airey D, Nwosu S, Perati PR, Tavori H, et al. Angiotensin-induced abdominal aortic aneurysms in hypercholesterolemic mice: role of serum cholesterol and temporal effects of exposure. PLoS ONE. 2014; 9:e84517. [PubMed: 24465413]
43. Wei S, Zhang Y, Su L, He K, Wang Q, Zhang Y, et al. Apolipoprotein E-deficient rats develop atherosclerotic plaques in partially ligated carotid arteries. Atherosclerosis. 2015 Dec.243:589–592. [PubMed: 26545012]
44. Saraff K, Babamusta F, Cassis LA, Daugherty A. Aortic dissection precedes formation of aneurysms and atherosclerosis in angiotensin II-infused, apolipoprotein E-deficient mice. Arterioscler Thromb Vasc Biol. 2003 Sep 1.23:1621–1626. [PubMed: 12855482]
45. Li Q, Dale WE, Hasser EM, Blaine EH. Acute and chronic angiotensin hypertension: neural and nonneural components, time course, and dose dependency. Am J Physiol. 1996 Jul.271:R200–7. [PubMed: 8760221]
46. Cassis LA, Marshall DE, Fettinger MJ, Rosenbluth B, Lodder RA. Mechanisms contributing to angiotensin II regulation of body weight. Am J Physiol. 1998 May.274:E867–76. [PubMed: 9612245]
47. Simon G, Abraham G, Cserep G. Pressor and subpressor angiotensin II administration. Two experimental models of hypertension. Am J Hypertens. 1995 Jun.8:645–650. [PubMed: 7662251]
48. Nickenig G, Jung O, Strehlow K, Zolk O, Linz W, Scholkens BA, et al. Hypercholesterolemia is associated with enhanced angiotensin AT1-receptor expression. Am J Physiol. 1997 Jun. 272:H2701–7. [PubMed: 9227549]
49. Daugherty A, Cassis L. Angiotensin II-mediated development of vascular diseases. Trends Cardiovasc Med. 2004 Apr.14:117–120. [PubMed: 15121160]
50. Katsuda S-I, Waki H, Yamasaki M, Nagayama T, O-Ishi H, Katahira K, et al. Postnatal changes in the rheological properties of the aorta in Sprague-Dawley rats. Exp Anim. 2002 Jan.51:83–93. [PubMed: 11871157]
51. Wolinsky H. Response of the rat aortic media to hypertension. Morphological and chemical studies. Circ Res. 1970 Apr.26:507–522. [PubMed: 5435712]
52. Xiong F, Zhao J, Zeng G, Huang B, Yuan D, Yang Y. Inhibition of AAA in a rat model by treatment with ACEI perindopril. J Surg Res. 2014 Jun 1.189:166–173. [PubMed: 24602481]
53. Su EJ, Lombardi DM, Siegal J, Schwartz SM. Angiotensin II induces vascular smooth muscle cell replication independent of blood pressure. Hypertension. 1998 Jun.31:1331–1337. [PubMed: 9622150]
54. Cao Z, Dean R, Wu L, Casley D, Cooper ME. Role of angiotensin receptor subtypes in mesenteric vascular proliferation and hypertrophy. Hypertension. 1999 Sep.34:408–414. [PubMed: 10489386]
55. Knipp BS, Ailawadi G, Sullivan VV, Roelofs KJ, Henke PK, Stanley JC, et al. Ultrasound measurement of aortic diameters in rodent models of aneurysm disease. J Surg Res. 2003 Jun 1.112:97–101. [PubMed: 12873440]

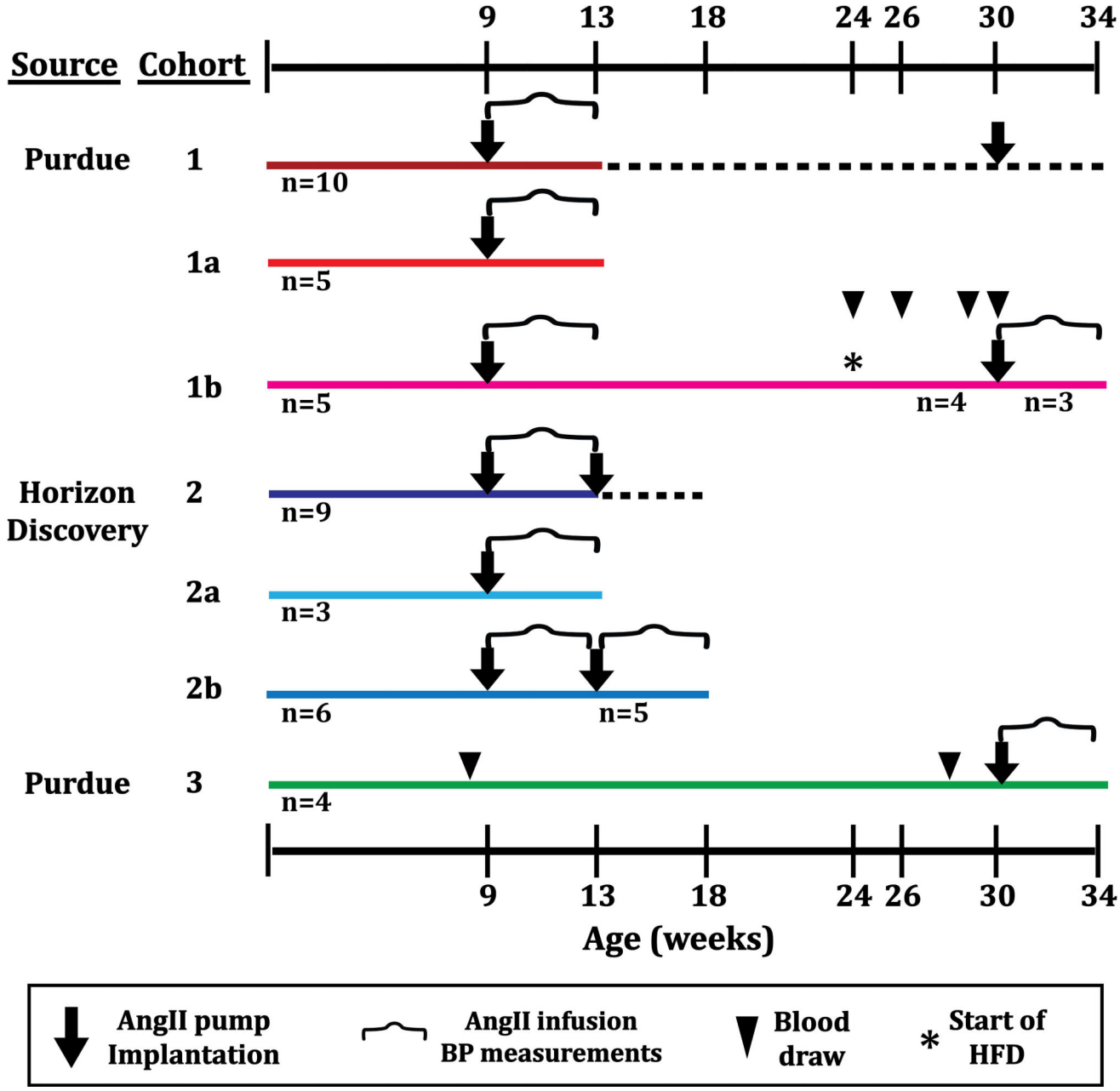

Figure 1. Schematic of study cohorts

Age and number of animals, time of pump implantation, periods for AngII infusion and blood pressure (BP) measurements, time points for blood collection, and start of high-fat diet (HFD) administration are indicated for each cohort. Animal sacrifices were carried out at the point where the line ends along each row. Two animals died unexpectedly after the start of the HFD (Cohort 1b) and one animal died after six weeks of continuous AngII infusion (Cohort 2b).

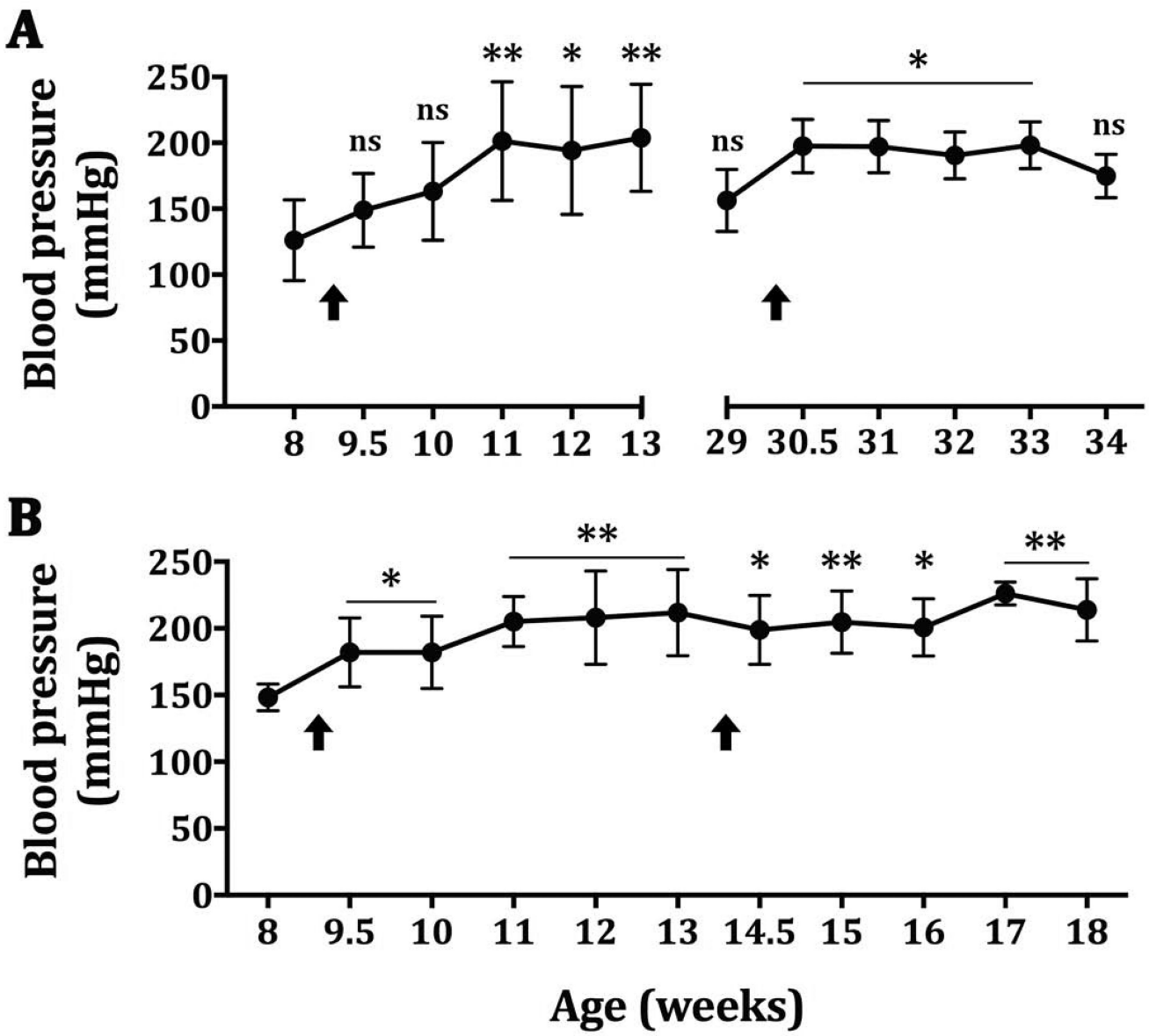

Figure 2. Systolic blood pressure measurements

All cohorts show a statistically significant elevation in systolic blood pressure (SBP) after AngII pump implantation (arrows). **A.** SBP for Cohort 1 (weeks 8 to 13) and Cohorts 1b and 3 (weeks 29 to 34). **B.** SBP for Cohort 2a (weeks 8 to 13) and Cohort 2b (weeks 13 to 18). S1 Table shows all individual data points for systolic, diastolic, and mean arterial blood pressure measurements.

* (p<0.05), ** (p<0.001), ns (no significance) relative to baseline (one-way ANOVA with Dunnett's multiple comparisons test)

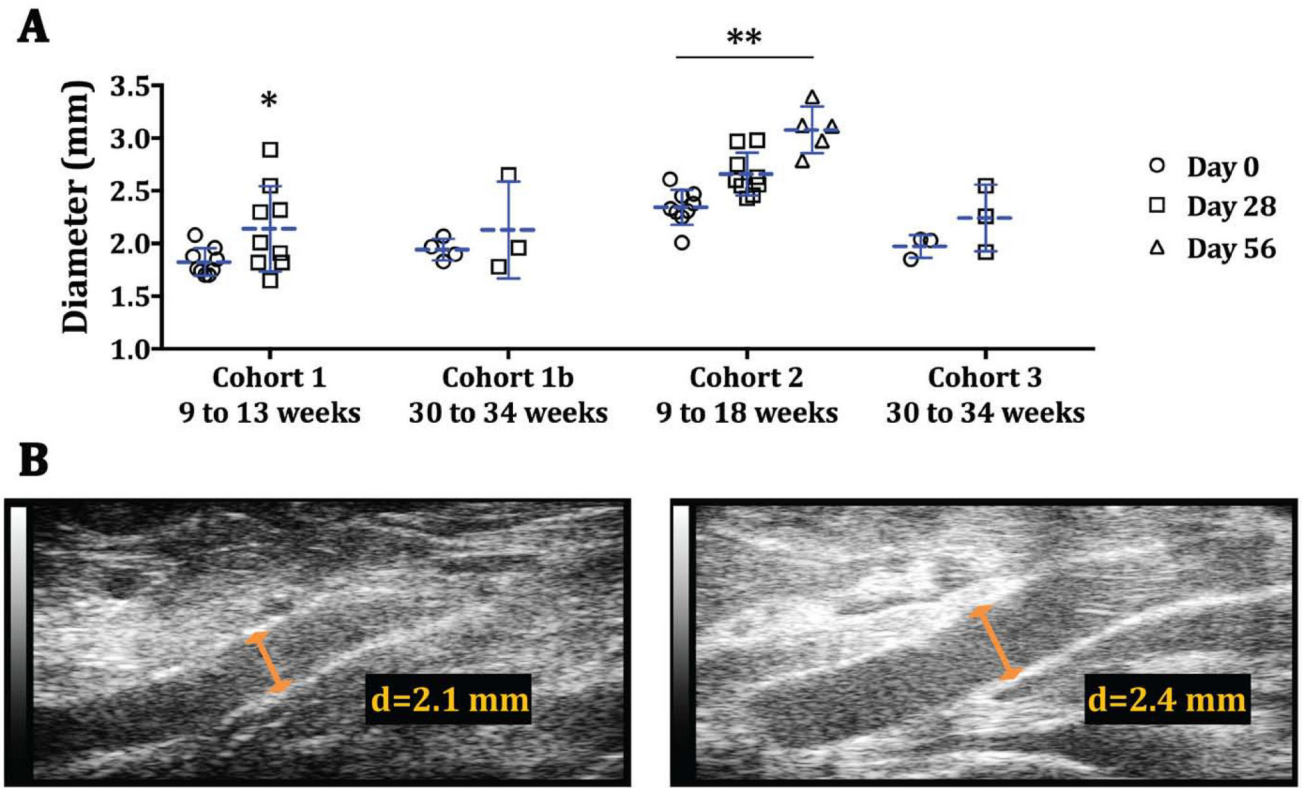

Figure 3. Suprarenal aortic diameter measurements

A. Mean suprarenal aortic diameter increased over 28 or 56 days of AngII infusion. These changes were significant for Cohorts 1 and 2 but not for Cohorts 1b (p=0.45) and 3 (p=0.18). One animal in Cohort 1b died between implantation and sacrifice. **B.** Representative long-axis B-mode images at days 0 and 28 for an animal in Cohort 3.

* (p<0.05), ** (p<0.001) relative to day 0 (Student's t-test; Kruskal-Wallis test with Dunn's multiple comparisons test)

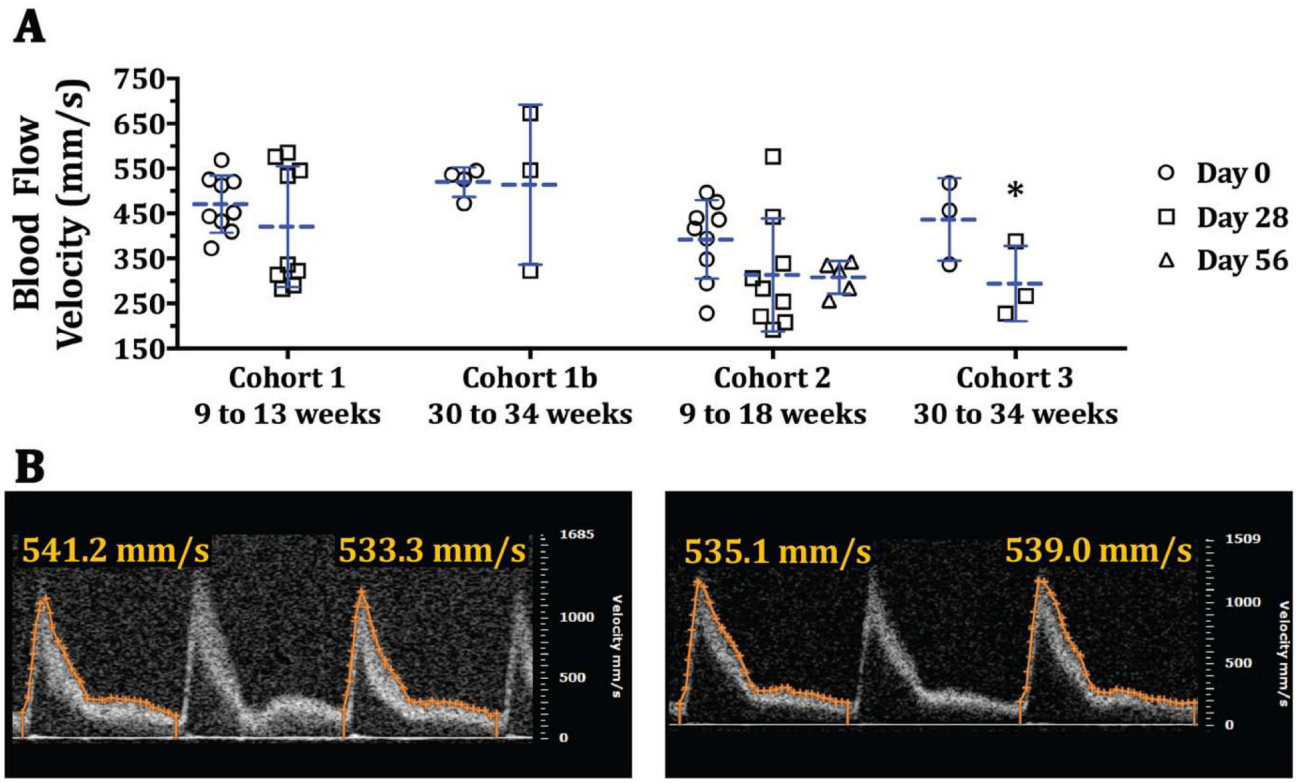

Figure 4. Suprarenal blood flow velocity measurements

A. Mean blood flow velocity did not change significantly after 28 or 56 days of AngII infusion ($p>0.05$) except in Cohort 3. One animal in Cohort 1b died between implantation and sacrifice. **B**. Representative PW Doppler images at days 0 and 28 for an animal in Cohort 1b.

* $p<0.05$ relative to day 0 (Student's t-test)

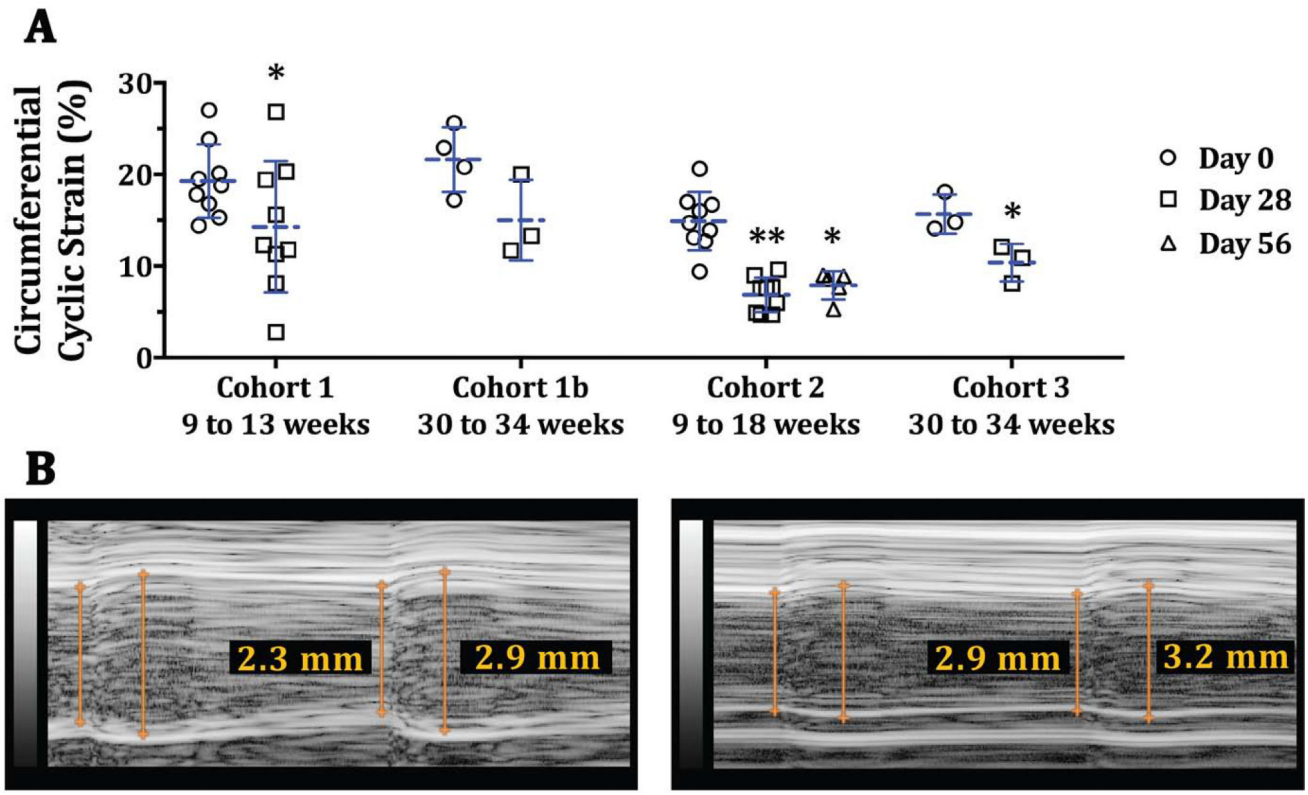

Figure 5. Suprarenal aortic circumferential cyclic strain measurements

A. Suprarenal aortic circumferential cyclic strain significantly decreased after 28 days of AngII infusion in all cohorts except Cohort 1b (p=0.077). Circumferential cyclic strain for Cohort 2b remained significantly reduced after 56 days. One animal in Cohort 1b died between implantation and sacrifice. **B.** Representative M-mode traces at days 0 and 28 for an animal in Cohort 1b.

* (p<0.05), ** (p<0.001) relative to day 0 (Student's t-test; Kruskal-Wallis test with Dunn's multiple comparisons test)

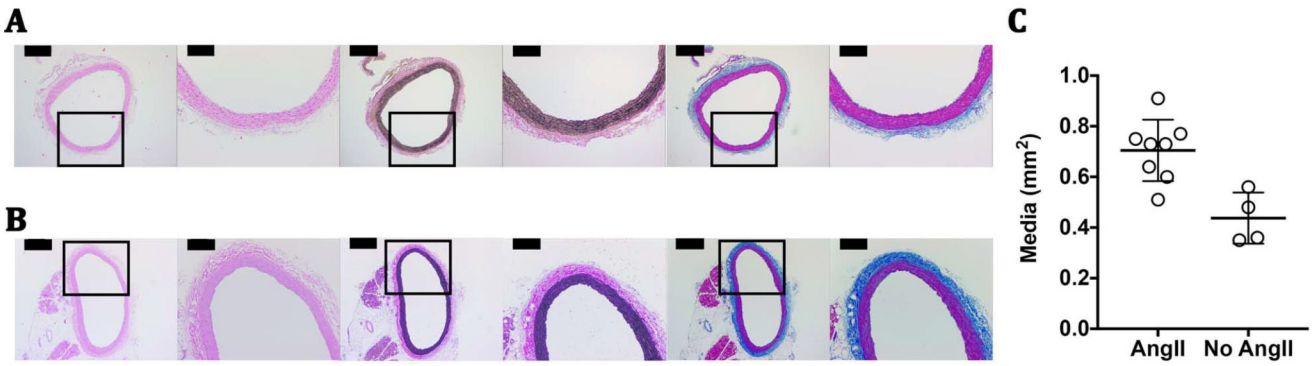

Figure 6. Histology and quantitative analysis of aortas from rats infused and not infused with AngII

H&E- (left), VVG- (middle), and MTC- (right) stained sections of suprarenal aortas from a rat in Cohort 3 (**A**) and a rat not infused with AngII (**B**). Boxes mark the magnified view of each section shown to the right. Scale bars: 500 μm (4X magnification) and 200 μm (10X magnification). The mean cross-sectional area of the media (**C**) of the suprarenal aortas of AngII-infused rats (n=8; age: 6.7±2.8 months; mass: 368±53.5 g) was 1.6-fold greater (*, p=0.0036) than for rats not infused with AngII (n=4; age: 4.3±1.9 months; mass: 378±83.2 g).

Table 1

Average blood serum cholesterol values.

Cohort	Age (weeks)	Diet	Serum cholesterol (mg/dL)	n	Significance
Wildtype	8	Normal	104.7 ± 14.2	4	
1b	24	Normal	190.5 ± 13.4	5	*
1b	26	Atherogenic	267.5 ± 10.3	5	*, °
1b	29	Atherogenic	203.4 ± 5.2	4	*, #
1b	30	Atherogenic	236.6 ± 8.9	4	*, °, #, ^
3	8	Normal	147.7 ± 8.4	5	*
3	28	Normal	136.1 ± 5.5	5	*

Values are presented as mean ± SD

* $p<0.01$ relative to wildtype animals (one-way ANOVA with Dunnett's test)

$p<0.05$ (one-way ANOVA with Tukey HSD post-hoc) for comparisons within Cohort 1b:

° before HFD (24 weeks of age)

after start of HFD (26 weeks of age)

^ after start of HFD (at 29 weeks of age)